YAWING MOMENT COEFFICIENT FOR PLAIN AILERONS AT SUBSONIC SPEEDS

1. NOTATION AND UNITS (see Sketch 1.1)

		SI	*British*
A	aspect ratio		
b	wing span	m	ft
C_L	lift coefficient of wing and flap system with ailerons undeflected, $L/\frac{1}{2}\rho V^2 S$		
ΔC_{Lf}	component of lift coefficient due to deployment of trailing-edge flaps		
C_l	rolling moment coefficient due to ailerons, $\mathscr{L}/\frac{1}{2}\rho V^2 Sb$		
C_n	yawing moment coefficient due to ailerons, $\mathscr{N}/\frac{1}{2}\rho V^2 Sb$		
C_{ni}	contribution to C_n due to changes in induced drag		
C_{np}	contribution to C_n due to changes in profile drag		
c_f/c	ratio of aileron chord aft of hinge line to local wing chord at mid-span of aileron		
$F(\eta)$	function defining C_{ni} for ailerons that extend from η to wing tip		
G	function in calculation of C_{ni} see Equation (2.3) and Figure 1		
H	function in calculation of C_{ni} see Equation (2.3) and Figure 2	deg^{-1}	deg^{-1}
J_f	empirical factor for converting ΔC_{Lf} into effective twist angle in calculation of C_{ni} see Equation (2.3). Taken as 18.0 degrees	degree	degree
J_δ	empirical factor applied to δ_t in calculation of C_{ni} see Equation (2.3). Taken as 1.4		
L	lift	N	lbf
$\mathscr{L}$	rolling moment, positive starboard wing down	N m	lbf ft
$L_{\xi'}$	rolling moment derivative with respect to ξ', $\partial C_l/\partial\xi'$ for ailerons that extend from η to wing tip	rad^{-1}	rad^{-1}
M	Mach number		
$\mathscr{N}$	yawing moment, positive nose to starboard	N m	lbf ft

S	wing planform area	m^2	ft^2
s	wing semispan	m	ft
V	free-stream velocity	m/s	ft/s
β	compressibility parameter $(1 - M^2)^{½}$		
γ'	angle between chord line of aerofoil section and line joining mid-thickness point at hinge line to trailing edge of undeflected aileron, measured at mid-span of aileron in plane normal to hinge line	degree	degree
δ_t	geometric twist angle of wing tip relative to root chord, positive leading-edge up	degree	degree
η	spanwise distance from wing centre-line as fraction of semispan		
η_i	value of η at inboard limit of aileron at hinge line		
η_o	value of η at outboard limit of aileron at hinge line		
$\bar{\eta}$	$(\eta_i + \eta_o)/2$		
λ	wing taper, ratio of tip chord to centre-line chord		
$\Lambda_{¼}$	sweepback of wing quarter-chord line	degree	degree
$\Lambda_{½}$	sweepback of wing half-chord line (needed in calculation of $L_{\xi'}$)	degree	degree
Λ_h	sweepback of control hinge line	degree	degree
μ	part-span factor in calculation of C_{np}, see Figure 3		
μ_i ,μ_o	values of μ at η_i and η_o, respectively		
ξ'	aileron deflection angle measured in plane normal to hinge line, arithmetic mean of deflection angles of port and starboard ailerons, positive for starboard aileron down and port aileron up, $½(\xi'_p + \xi'_s)/57.3$	radian	radian
ξ'_p	deflection of port aileron measured in plane normal to hinge line, positive trailing-edge up	degree	degree
ξ'_s	deflection of starboard aileron, measured in plane normal to hinge line, positive trailing-edge down	degree	degree
ρ	free-stream density of air	kg/m^3	$slug/ft^3$

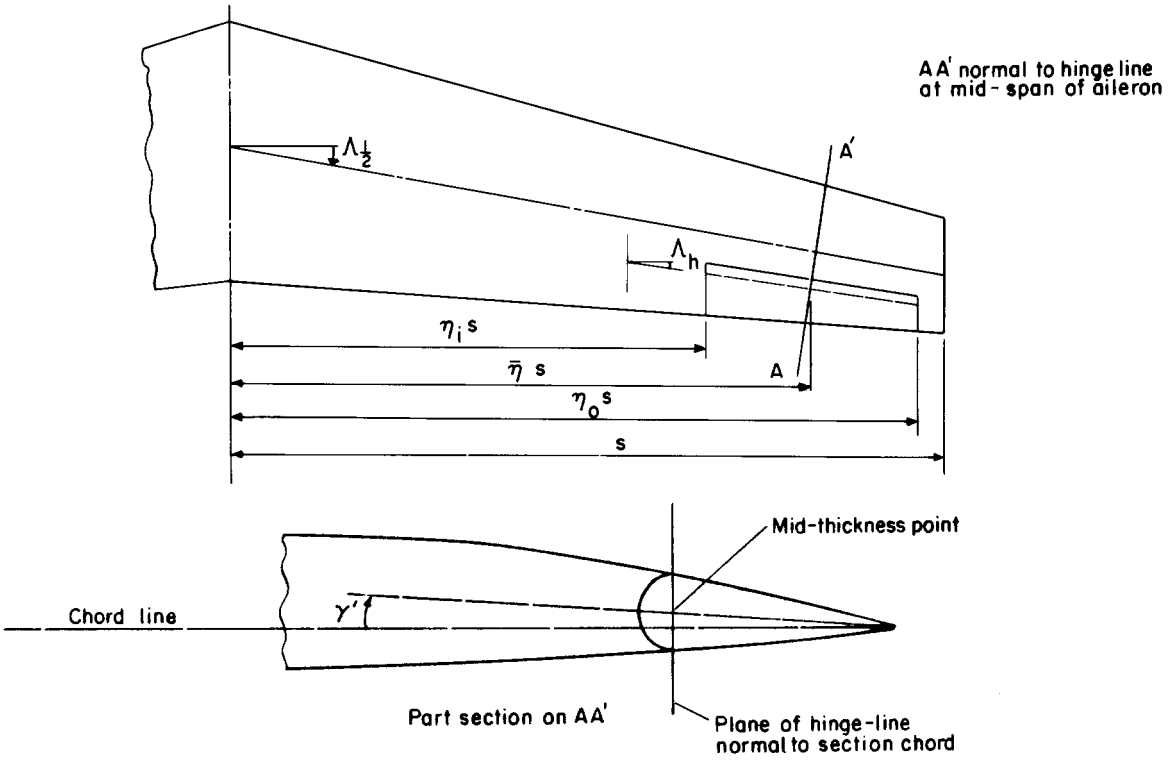

Sketch 1.1 Wing and aileron geometry

2. METHOD*

This Item presents a semi-empirical method for predicting the yawing moment coefficient C_n due to the operation of plain sealed ailerons at subsonic free-stream Mach numbers when the flow over the wing is wholly subsonic. The coefficient is treated as the sum of two components, C_{ni} and C_{np}. The first is due to the asymmetric changes in induced drag caused by aileron deflection, and the second is due to imbalance of the profile drag on the port and starboard wings. Thus the total C_n is

$$C_n = C_{ni} + C_{np}\,. \tag{2.1}$$

2.1 Induced Drag Contribution

Theoretical considerations of the interaction of the symmetric wing loading due to angle of attack and the antisymmetric loading due to equally deflected ailerons (*e.g.* see Derivations 5 and 6), show that for a plane wing C_{ni} is proportional to the product of the wing lift coefficient C_L and the aileron rolling moment coefficient C_l $(= L_{\xi'})$. Derivation 6 goes on to show that if the ailerons are deflected unequally, so that $\xi'_p > \xi'_s$ say, then the appropriate symmetrical loading is for the wing with both ailerons raised by an angle $\frac{1}{2}[\xi'_p - \xi'_s]$. The change in C_{ni} depends on the consequent reduction in lift and is obtained theoretically as a contribution that is proportional to C_l, $\frac{1}{2}[\xi'_p - \xi'_s]$, and $1/A$ to a very good approximation. Other terms are necessary to account for any geometric twist of the wing and any deployment of trailing-edge flaps inboard of the ailerons. These considerations enable C_{ni} for ailerons extending from η_i to η_o be

* A FORTRAN computer program is available for the method of this Item and that of No.88013 as ESDUpac A8840, see Item No. 88040 for details.

expressed in the following form, which has been found to provide an excellent qualitative model,

$$C_{ni} = F(\eta_i) - F(\eta_o), \tag{2.2}$$

where

$$F(\eta) = -GC_L L_{\xi'}\xi' + \frac{H}{A}(\tfrac{1}{2}[\xi'_p - \xi'_s]\cos\Lambda_h - J_\delta\delta_t + J_f\Delta C_{Lf})L_{\xi'}\xi'. \tag{2.3}$$

For the particular case of ailerons that extend to the wing tip, $\eta_o = 1$, $F(1) = 0$ and so $C_{ni} = F(\eta_i)$.

The function G has been determined empirically from wind-tunnel data (Derivations 7 to 30) for the rate of change of $C_{ni}/(-L_{\xi'}\xi')$ with C_L, the lift coefficient of the wing and flap system with ailerons undeflected. Figures 1a, 1b and 1c present G plotted against $1/\beta A$ and η for $\lambda = 1.0$, 0.5 and 0.2, respectively; a cross plot against λ must be made to obtain G at intermediate values of λ. The carpets are comparable in form to the low-speed theoretical results of Derivations 5 and 6, but their empirical nature results in some modest adjustments. In particular there is a somewhat faster decrease in G with decreasing λ for wings of moderate or high aspect ratio. An allowance for compressibility effects has been made by the introduction of the reduced aspect ratio, βA in place of A.

The rolling moment derivative $L_{\xi'}$ for ailerons that extend from η to the wing tip can be calculated by the method of Item No. 88013 (Derivation 4) or experimental values may be substituted if they are available. Note that $L_{\xi'}$, is defined per radian and that ξ' is correspondingly in radians. The other angles in Equation (2.3) are in degrees.

The theoretical function H is given in Figure 2 in terms of λ and η, and has been reproduced from Derivation 6. The angle $\frac{1}{2}[\xi'_p - \xi'_s]\cos\Lambda_h$ allows for unequal (differential) operation of the ailerons measured in a streamwise plane. The influence of geometric twist is taken as the product of an empirical factor J_δ and the relative tip to root twist δ_t. The effect of flap deployment is modelled as an effective twist equal to the product of an empirically determined factor J_f and the component of the lift coefficient due to the flaps ΔC_{Lf}. Comparisons with experimental data (Derivations 22 to 30) showed that no empirical modification of the function H was necessary and that for a sufficient accuracy of prediction J_δ could be taken as 1.4 and J_f as 18.0 degrees. General values of J_δ and J_f have been left in Equation (2.3) as an aid to modelling experimental data. The terms that involve H are influenced by compressibility effects only through any changes in $L_{\xi'}$, and ΔC_{Lf}.

The component of C_{ni} that depends on C_L acts in an adverse manner in that it opposes the direction of the turn expected to accompany the roll produced by the ailerons. For a given aileron rolling moment the remaining terms give constant increments in the opposite sense if the ailerons are trailing-edge up relative to the inboard part of the wing. Thus at constant C_L a greater deflection of the up-going aileron, root-to-tip washout, or flap deployment all provide favourable contributions that will reduce and may overcome the adverse yawing moment. Conversely, if the ailerons are trailing-edge down the adverse yawing moment will increase.

2.2 Profile Drag Contribution

The profile drag contribution C_{np} is estimated by using the method given in Item No. 87024 (Derivation 3) for estimating the drag coefficient increment due to full-span plain flaps at constant lift, together with a part-span factor from Item No. Aero F.02.01.07 (Derivation 1) to allow for the limited extent of the ailerons, and then taking a moment arm $\bar{\eta}s$ on the assumption that the drag acts at the mid-span of the ailerons. The data in Item No. 87024 are provided with convenient mathematical expressions and, with some

rearrangement into a general form for small aileron deflections, this allows C_{np} to be written

$$C_{np} = (\mu_i - \mu_o)\frac{\bar{\eta}}{4}\frac{c_f}{c}\cos\Lambda_{¼}\cos^2\Lambda_h\left\{\left[1 - [0.05\gamma'\cos\Lambda_h]^2\left[1 - \frac{|\xi'_s|}{\xi'_s}\right]\right]\left(\frac{\gamma' + \xi'_s}{57.3}\right)^2\right.$$
$$\left. - \left[1 - [0.05\gamma'\cos\Lambda_h]^2\left[1 + \frac{|\xi'_p|}{\xi'_p}\right]\right]\left(\frac{\gamma' - \xi'_p}{57.3}\right)^2\right\}. \qquad (2.4)$$

The part-span factor μ is given in Figure 3 as a function of η and λ; μ_i and μ_o are the values of μ that apply at η_i and η_o respectively. In Equation (2.4), c_f/c is the ratio of aileron chord to local wing chord at the mid-span of the aileron. All angles are in degrees. The expressions that involve $0.05\gamma'$ allow for the the fact that the profile drag of the up-going aileron is reduced by any aft camber of the wing, see Item No. 87024. The angle γ' is measured at the mid-span of the aileron. The method in Item No. 87024 makes no allowance for the effects of compressibility, but this simplification is unlikely to introduce unacceptable errors in the estimation of C_n.

For wings with $\gamma' = 0$ and equal deflection of the ailerons the changes in profile drag on the port and starboard wings are equal and $C_{np} = 0$. If $\gamma' = 0$ and the up-going aileron is deflected more than the down-going aileron then C_{np} provides a small favourable yawing moment. If γ' is increased in this situation C_{np} first decreases in magnitude and then changes sign to give an adverse yawing moment.

3. ACCURACY AND APPLICABILITY

3.1 Accuracy

Comparisons with the experimental data of Derivations 7 to 30 suggest that at $C_L = 0$, C_n/ξ' is predicted to within about ± 0.003 rad^{-1} for wings with no flaps deployed. This provides a measure of the accuracy of prediction of the combined contributions from unequal aileron deflection, wing geometric twist and changes in profile drag. It will also reflect any effect of distortion of the wing loading due to the presence of a fuselage or any engine nacelles. The function G predicts the rate of change of $C_n/(-L_{\xi'}\xi')$ with C_L to within about ± 0.02. The scatter encountered in the determination of J_δ was about ± 0.4 and for J_f it was about ± 2.5 degrees.

3.2 Applicability

For ailerons that extend to near the wing tip, $\eta_o \geq 0.9$, Table 3.1 indicates according to the range of aspect ratio the combinations of geometric parameters over which the method has been tested against experimental data. Geometric twist angles in the range $-3° \leq \delta_t \leq 0$ were covered. Data for wings with flaps deployed were studied for wings with $A \geq 5$ and flaps that extended from close to the fuselage side to near the inboard end of the ailerons with flap lift coefficient components in the range $0.4 \leq \Delta C_{Lf} \leq 1.4$. Only a small number of experimental data were available for inboard ailerons with $\eta_o \leq 0.5$, but satisfactory estimates were obtained in those cases. The method should be used only for plain ailerons that are sealed or have so small a control gap that they are effectively sealed.

The method applies directly to straight-tapered wings. Its use may be extended to wings with other planforms, e.g. cranked wings, by first employing the geometric techniques in Appendix A of Item No. 76003 (Derivation 2) to construct an "equivalent" straight-tapered wing to provide suitably representative values of A, λ, $\Lambda_{¼}$ and $\Lambda_{½}$.

The method will apply over the part of the lift curve where C_L increases linearly with angle of attack.

When predicting C_{ni} some allowance for a loss of control effectiveness at high angles of aileron deflection can be made by substituting experimental values of $L_{\xi'}$ in Equation (2.3), but the method will become less reliable and must be used with caution for $\xi' > 15°$. If only theoretical estimates of $L_{\xi'}$ are available the method should not be used for $\xi' > 15°$.

Virtually all of the experimental data used to verify the method were from tests at low speeds. Although it has not been possible to assess the accuracy thoroughly, comparisons with the few test cases that were available at high subsonic speeds suggest that acceptable estimates can be expected provided the flow over the wing remains wholly subsonic.

TABLE 3.1

Parameter	*Range*	*Range*	*Range*
A	2 to 4	5 to 9	10 to 12
λ *	0.5 to 1	0.3 to 1	0.4 to 1
$\Lambda_{½}$	0 to 45°	0 to 25°	0 to 5°
η_i	0 to 0.8	0.6 to 0.8†	0.6 to 0.7

* A single set of data was available for $\lambda = 0.2$, $A = 3$ and $\Lambda_{½} = 37°$ from Derivation 20. Those tests were conducted at high subsonic speeds ($M \geq 0.8$) but supported the supposition made when constructing the carpets for G that the effect of taper was small for wings of low aspect ratio.

† For $A = 6$, $\lambda = 1$ and $\Lambda_{½} = 0$ one set of data covered the range of η_i from 0 to 0.8.

4. DERIVATION

The Derivation lists selected sources that have assisted in the preparation of this Item.

ESDU Items

1. ESDU — Conversion factor for profile drag increment for part-span flaps. Item No. Aero F.02.01.07, ESDU International, June 1944.

2. ESDU — Geometric properties of cranked and straight-tapered wing planforms. Item No. 76003, ESDU International, January 1976.

3. ESDU — Low-speed drag coefficient increment at constant lift due to full-span plain flaps. Item No. 87024, ESDU International, November 1987.

4. ESDU — Rolling moment derivative, L_{ξ}, for plain ailerons at subsonic speeds. Item No. 88013, ESDU International, August 1988.

Theoretical Studies

5. PEARSON, H.A. — Theoretical span loading and moments of tapered wings produced by aileron deflection. NACA tech. Note 589, 1935.

6. WEICK, F.E.
JONES, R.T. — Résumé and analysis of NACA lateral control research. NACA Rep. 605, 1937.

Wind-tunnel Data

7. LETKO, W. GOODMAN, A. — Preliminary wind-tunnel investigation at low speed of stability and control characteristics of swept-back wings. NACA tech. Note 1046, 1946.

8. SCHULDENFREI, M. COMISAROW, P. — Stability and control characteristics of an airplane model having a 45.1° swept-back wing with aspect ratio 2.50 and taper ratio 0.42 and a 42.8° swept-back horizontal tail with aspect ratio 3.87 and taper ratio 0.49. NACA RM L7B25 (TIL 1389), 1947.

9. SPOONER, S.H. WOODS, R.L — Low-speed investigation of aileron and spoiler characteristics of a wing having 42° sweepback of the leading edge and circular-arc airfoil sections at Reynolds numbers of approximately 6.0 $\times 10^6$. NACA RM L9A07 (TIL 2108), 1949.

10. BOLLECH, T.V. PRATT, G.L. — Investigation of low-speed aileron control characteristics at a Reynolds number of 6,800,000 of a wing with leading edge swept back 42° with and without high lift devices. NACA RM L9E24 (TIL 2164), 1949.

11. NAESETH, R.L. O'HARE, W.M. — The effect of aileron span and spanwise location on the low-speed lateral control characteristics of an untapered wing of aspect ratio 2.09 and 45° sweepback. NACA RM L9L09a (TIL 2355), 1950.

12. PASAMANICK, J. SELLERS, B.T. — Low-speed investigation of the effect of several flap and spoiler ailerons on the lateral characteristics of a 47.5° sweptback-wing-fuselage combination at a Reynolds number 4.4×10^6. NACA RM L50J20 (TIL 2713), 1950.

13. HADAWAY, W.M. SALMI, R.J. — Investigation of low-speed lateral control and hinge-moment characteristics of a 20-percent-chord plain aileron on a 47.7° sweptback wing of aspect ratio 5.1 at a Reynolds number of 6.0×10^6. NACA RML51F22 (TIL 2918), 1951.

14. FITZPATRICK J.E. WOODS, R.L. — Low speed lateral-control characteristics of an unswept wing with hexagonal airfoil sections and aspect ratio 2.5 equipped with spoilers with sharp- and thickened-trailing-edge flap-type ailerons at a Reynolds number of 7.6×10^6. NACA RM L52B15 (TIL 3100), 1952.

15. FISCHEL, J. NAESETH, R.L. HAGERMAN, J.R. O'HARE, W.M. — Effect of aspect ratio on the low-speed lateral control characteristics of untapered low-aspect-ratio wings equipped with flap and with retractable ailerons. NACA Rep. 1091, 1952.

16. HADAWAY, W.M. — Low-speed lateral control characteristics of an unswept wing with hexagonal airfoil sections and aspect ratio 4.0 at a Reynolds number of 6.2×10^6. NACA RM L53A29 (TIL 3675), 1953.

17. CANCRO, P.A. — Low-speed aileron effectiveness as determined by force tests and visual-flow observations on a 52° sweptback wing with and without chord-extensions. NACA RM L53B26 (TIL 3720), 1953.

18. MOSELEY, W.C. TAYLOR, R.T. — Low-speed static stability and control characteristics of a ¼-scale model of the Bell X-1 airplane equipped with a 4-percent-thick, aspect-ratio-4, unswept wing. NACA RM L53H27 (TIL 3941), 1953.

19. VOGLER, R.D. — Wind-tunnel investigation at high subsonic speeds of jet, spoiler and aileron control on a 1/16-scale model of the Douglas D-558-II research airplane. NACA RM L56E25 (TIL 5192), 1956.

20. HIESER, G.; WHITCOMB, C.F. — Effectiveness at transonic speeds of flap-type ailerons for several spanwise locations on a 4-percent-thick sweptback-wing-fuselage model with and without tails. NACA RM L56J04 (TIL 5443), 1957.

21. TEPER, G.L. — Aircraft stability and control data. Systems Technology Inc. tech Rep 176-1, 1969.

22. FINK, M.P.; FREEMAN, D.C. — Full-scale wind-tunnel investigation of static longitudinal and lateral characteristics of a light twin-engine airplane. NASA tech. Note D-4983, 1969.

23. FINK, M.P.; FREEMAN, D.C. — Full-scale wind-tunnel investigation of static longitudinal and lateral characteristics of a light single-engine airplane. NASA tech. Note D-5700, 1970.

24. SHIVERS, J.P.; FINK, M.P.; WARE, G.M. — Full-scale wind-tunnel investigation of static longitudinal and lateral characteristics of a light single-engine low-wing airplane. NASA tech. Note D-5857, 1970.

25. FINK, M.P.; SHIVERS, J.P.; SMITH, C.C. — A wind-tunnel investigation of static longitudinal and lateral characteristics of a full-scale mockup of a light twin-engine airplane. NACA tech. Note D-6238, 1971.

26. SODERMAN, P.T.; AIKEN, T.N. — Full-scale wind-tunnel test of a small unpowered jet aircraft with a T-tail. NASA tech. Note D-6573, 1971.

27. WOLOWICZ, C.H.; YANCEY, R.B. — Lateral-directional aerodynamic characteristics of light twin-engine, propeller-driven airplanes. NASA tech. Note D-6946, 1972.

28. BAe — Unpublished wind-tunnel data.

29. SHORT BROTHERS — Unpublished wind-tunnel data.

30. MBB — Unpublished wind-tunnel data.

5. EXAMPLE

Find the yawing moment coefficient as a function of lift coefficient for the plain sealed ailerons of the wing shown in Sketch 5.1 for a Mach number of 0.4. The port aileron is deflected 11.0° up and the starboard aileron 9.0° down. Also determine the effect of deployment of trailing-edge flaps inboard of the ailerons to give a lift coefficient component ΔC_{Lf} of 0.6.

Geometric parameters for wing	
$\xi'_p = +11.0°$	$A = 6.0$
$\xi'_s = +9.0°$	$\lambda = 0.5$
$\gamma' = 3.0°$	$\eta_i = 0.70$
$\Lambda_{¼} = 34.2°$	$\eta_o = 0.95$
$\Lambda_h = 29.7°$	$\bar{\eta} = 0.825$
$\delta_t = -2.0°$	$c_f/c = 0.25$

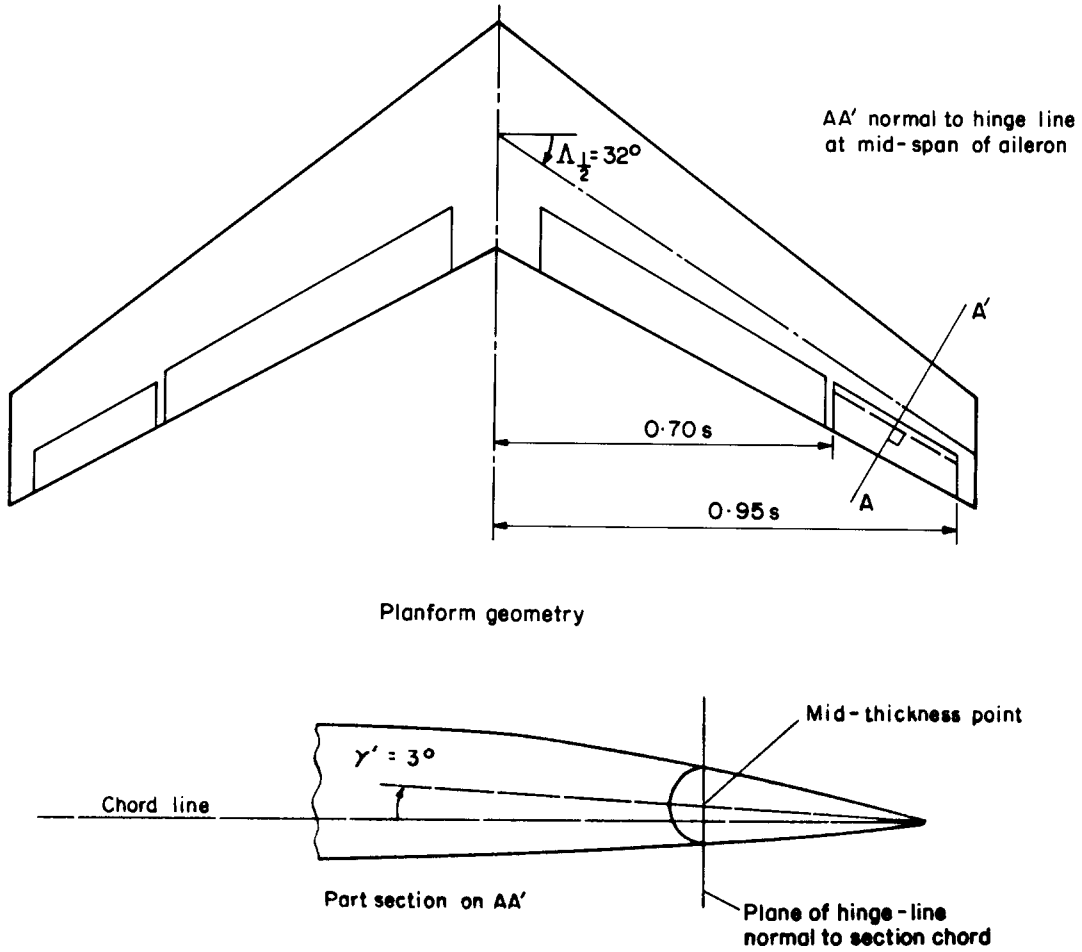

Sketch 5.1

(i) Calculation of induced drag component of C_n for wing without flap deployment

The Mach number is 0.4 so $\beta = (1-M^2)^{½} = (1-0.4^2)^{½} = 0.917$.

From Figure 1b for $\lambda = 0.5$ with $1/\beta A = 1/(0.917 \times 6.0) = 0.182$ and $\eta_i = 0.7$, $G = 0.212$.

(For a general value of λ it is necessary to cross plot between Figures 1a, 1b and 1c as in Sketch 5.2.)

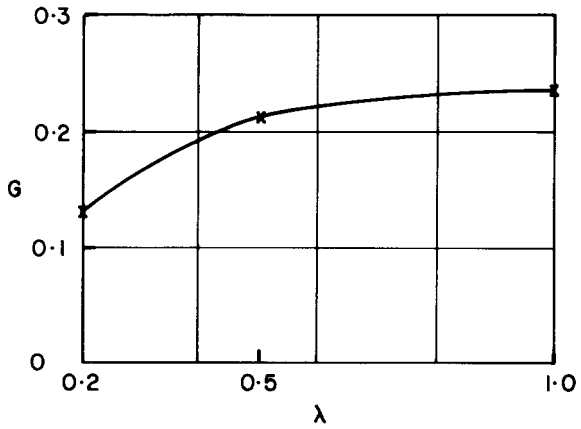

Sketch 5.2

From Figure 2, for $\lambda = 0.5$ and $\eta = 0.7$, $H = 0.0829$ deg^{-1}.

The wing in Sketch 5.1 has the same planform geometry and ailerons as that used in the worked example of Item No. 88013 where the Mach number is also 0.4. If the same section properties, and Reynolds number are also assumed then the predicted rolling moment derivative for ailerons that extend from $\eta = 0.7$ to the wing tip is $L_{\xi'} = -0.103 \text{rad}^{-1}$.

The aileron mean deflection angle $\xi'$is$½(\xi'_p + \xi'_s)/57.3 = ½(11 + 9)/57.3 = 0.175$ radians.

Substitution of the values calculated above into Equation (2.3) with $J_\delta = 1.4$ and $\Delta C_{Lf} = 0$ gives

$$F(0.7) = -GC_L L_{\xi'}\xi' + \frac{H}{A}(½[\xi'_p - \xi'_s]\cos\Lambda_h - J_\delta\delta_t)L_{\xi'}\xi'$$

$$= -0.212C_L(-0.103 \times 0.175) + \frac{0.0829}{6.0}(½[11-9]\cos 29.7° - 1.4 \times (-2))(-0.103 \times 0.175)$$

$$= 0.00382C_L - 0.00091.$$

A similar calculation for ailerons that extend from $\eta = 0.95$ to the wing tip, with $G = 0.255$, $H = 0.079$ deg^{-1}, and $L_{\xi'} = -0.009$ rad^{-1}, gives

$$F(0.95) = 0.00040\ C_L - 0.00008.$$

So for the ailerons of this example which extend from $\eta = 0.7$ to $\eta = 0.95$, Equation (2.2) gives

$$C_{ni} = F(0.7) - F(0.95)$$

$$= 0.00342C_L - 0.00083$$

(ii) Calculation of induced drag component of C_n with flap deployment

If trailing-edge flaps are deployed then from Equation (2.3) with J_f = 18.0 degrees the additional contribution to $F(0.7)$ is

$$\frac{H}{A}(J_f \Delta C_{Lf}) L_{\xi'} \xi' = \frac{0.0829}{6.0}(18.0 \Delta C_{Lf})(-0.103 \times 0.175) = -0.00448 \Delta C_{Lf},$$

so $$F(0.7) = 0.00382 C_L - 0.00091 - 0.00448 \Delta C_{Lf}.$$

Similarly, the additional contribution to F(0.95), with H = 0.079 deg^{-1} and $L_{\xi'}$ = –0.009 rad^{-1}, is $-0.00037 \Delta C_{Lf}$, so

$$F(0.95) = 0.00040 C_L - 0.00008 - 0.00037 \Delta C_{Lf}.$$

Therefore with flaps deployed

$$\begin{aligned} C_{ni} &= F(0.7) - F(0.95) \\ &= 0.00342 C_L - 0.00083 - 0.00411 \Delta C_{Lf}, \end{aligned}$$

which for ΔC_{Lf} = 0.6 becomes

$$\begin{aligned} C_{ni} &= 0.00342 C_L - 0.00083 - 0.0041 \times 0.6 \\ &= 0.00342 C_L - 0.00330. \end{aligned}$$

(iii) Calculation of profile drag component of C_n

From Figure 3 for $\lambda = 0.5$, $\mu = \mu_i = 0.220$ for $\eta = \eta_i = 0.7$, and $\mu = \mu_o = 0.035$ for $\eta = \eta_o = 0.95$.

Substitution in Equation (2.4) gives

$$\begin{aligned} C_{np} &= (\mu_i - \mu_o)\frac{\bar{\eta}}{4}\frac{c_f}{c}\cos\Lambda_{¼}\cos^2\Lambda_h \left\{ \left[1 - [0.05\gamma' \cos\Lambda_h]^2 [1 - \frac{|\xi'_s|}{\xi'_s}]\right]\left(\frac{\gamma' + \xi'_s}{57.3}\right)^2 \right. \\ &\quad \left. - \left[1 - [0.05\gamma' \cos\Lambda_h]^2 [1 + \frac{|\xi'_p|}{\xi'_p}]\right]\left(\frac{\gamma' - \xi'_p}{57.3}\right)^2 \right\} \\ &= (0.220 - 0.035)\frac{0.825}{4} \times 0.25 \times \cos 34.2° \cos^2 29.7 \left\{ \left[1 - [0.05 \times 3.0 \cos 29.7°]^2 [1 - \frac{|9.0|}{9.0}]\right] \right. \\ &\quad \left. \times \left(\frac{3.0 + 9.0}{57.3}\right)^2 - \left[1 - [0.05 \times 3.0 \cos 29.7°]^2 [1 + \frac{|11.0|}{11.0}]\right]\left(\frac{3.0 - 11.0}{57.3}\right)^2 \right\} \\ &= 0.00595 \left\{ \left[1 - [0.130]^2 [0]\right]\left(\frac{12.0}{57.3}\right)^2 - \left[1 - [0.130]^2 [2]\right]\left(\frac{-8.0}{57.3}\right)^2 \right\} \\ &= 0.00595 \times 0.0250 \\ &= 0.00015. \end{aligned}$$

(iv) Calculation of total C_n

The results of steps (*i*) to (*iii*) are added to give the total yawing moment coefficient. If trailing-edge flaps are not deployed

$$\begin{aligned} C_n &= C_{ni} + C_{np} \\ &= 0.00342C_L - 0.00083 + 0.00015 \\ &= 0.00342C_L - 0.00068, \end{aligned}$$

i.e. $C_n/\xi' = C_n/0.175 = 0.0195C_L - 0.0039 \text{ rad}^{-1}$

If trailing-edge flaps are deployed then

$$\begin{aligned} C_n &= C_{ni} + C_{np} \\ &= 0.00342C_L - 0.00330 + 0.00015 \\ &= 0.00342C_L - 0.00315, \end{aligned}$$

i.e $C_n/\xi' = 0.0195C_L - 0.0180 \text{ rad}^{-1}$.

Sketch 5.3 shows the results plotted in the form $C_n/\xi' \text{rad}^{-1}$ against C_L, the total lift coefficient of the wing and flap system.

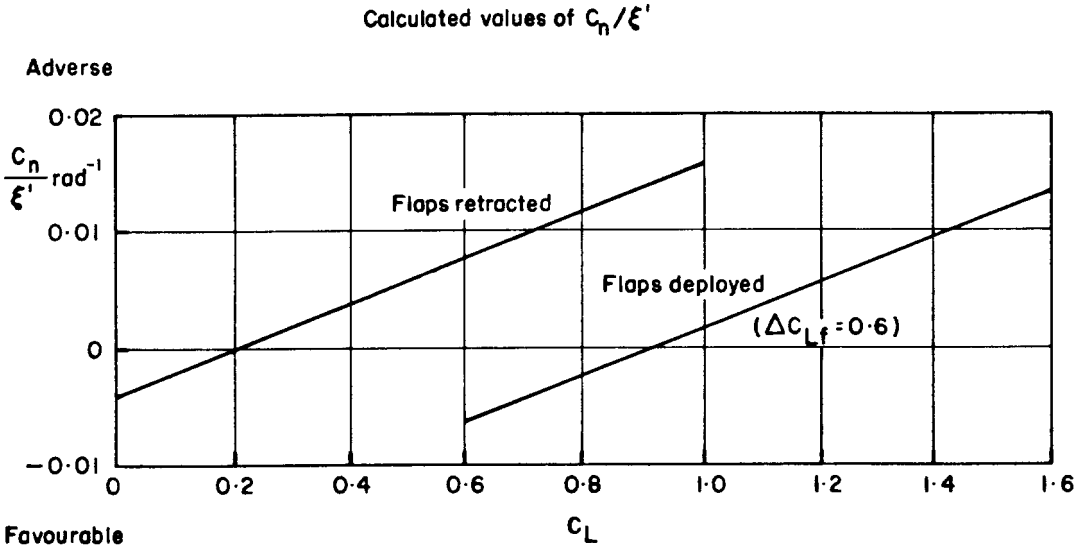

Sketch 5.3

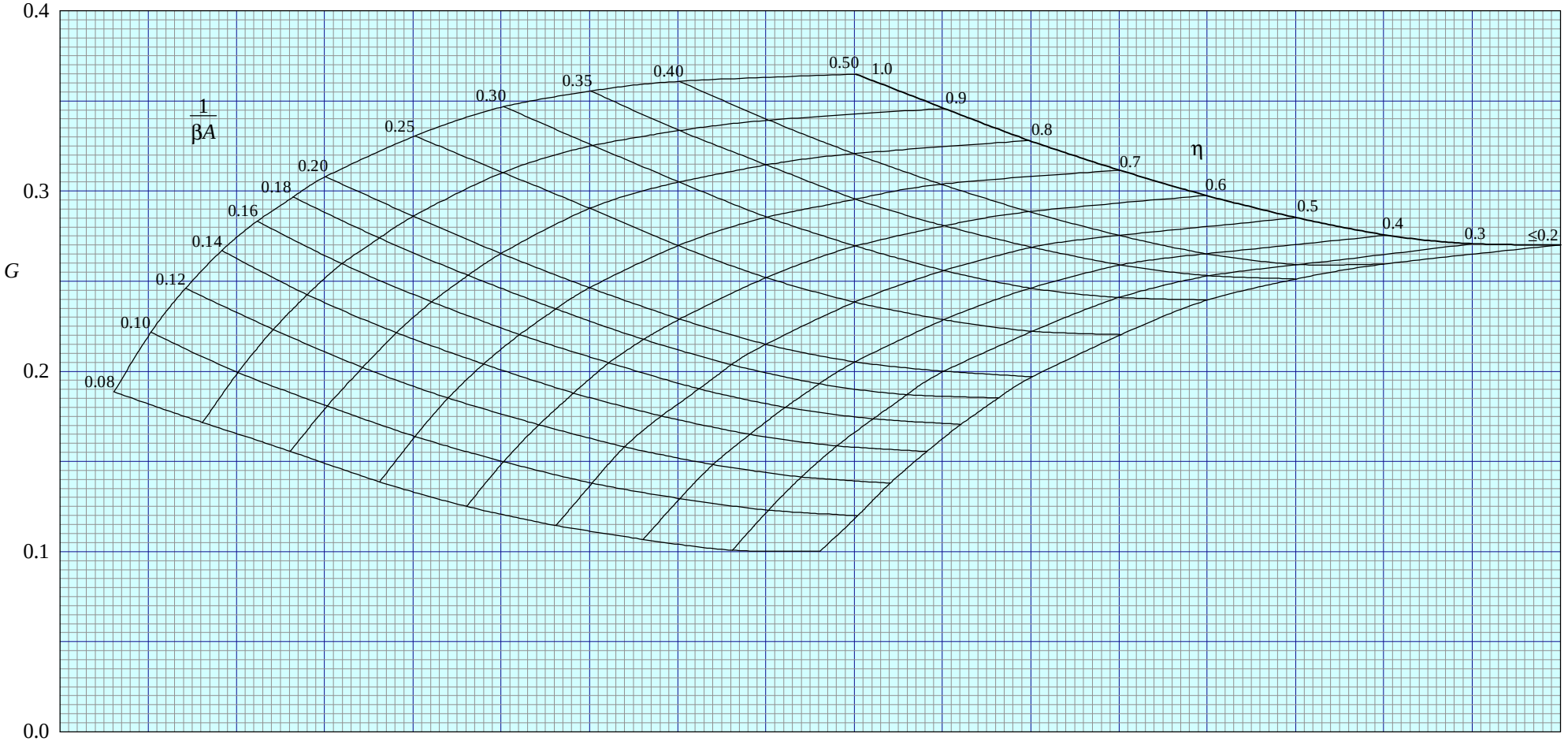

FIGURE 1a FUNCTION *G* FOR λ = 1.0

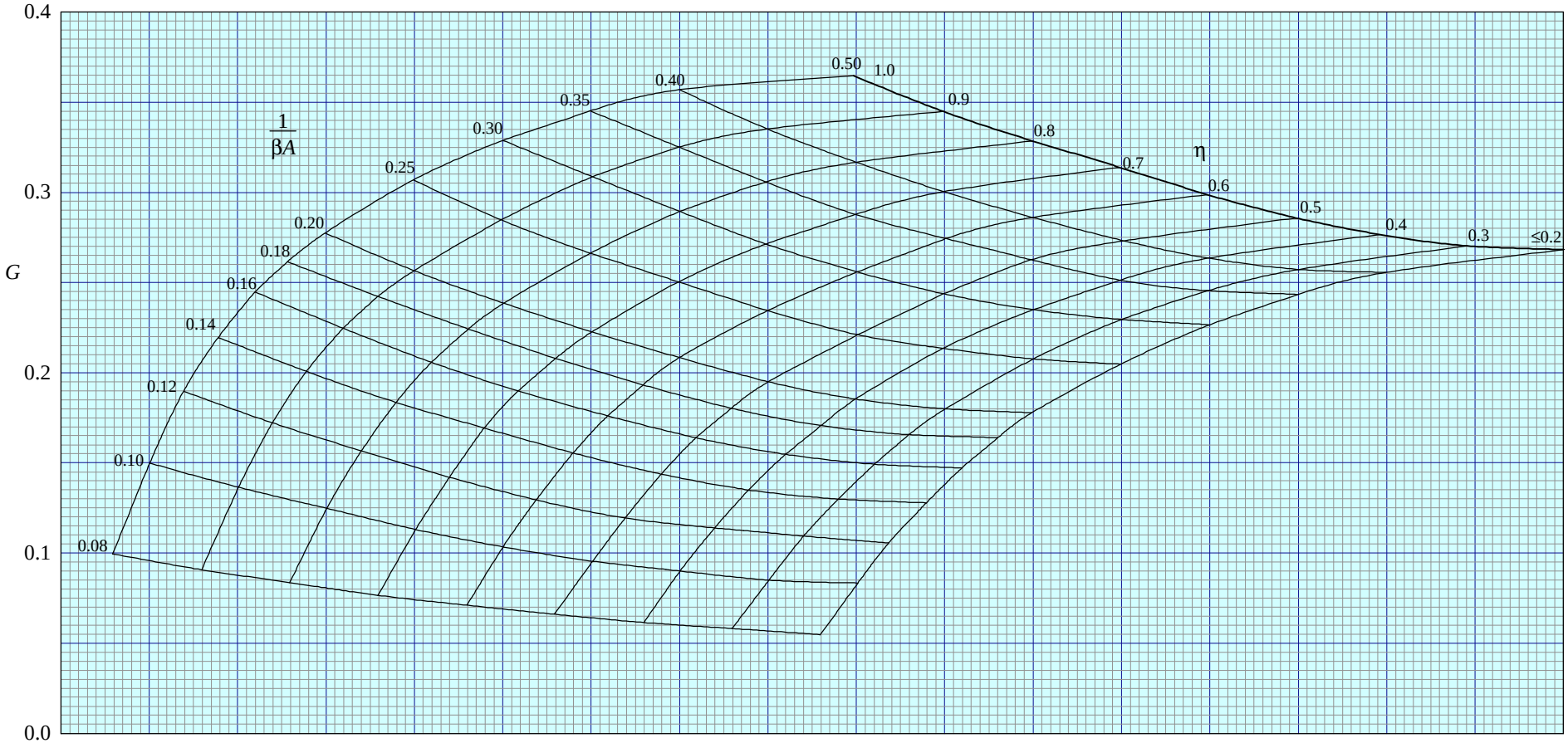

FIGURE 1b FUNCTION *G* FOR λ = 0.5

88029

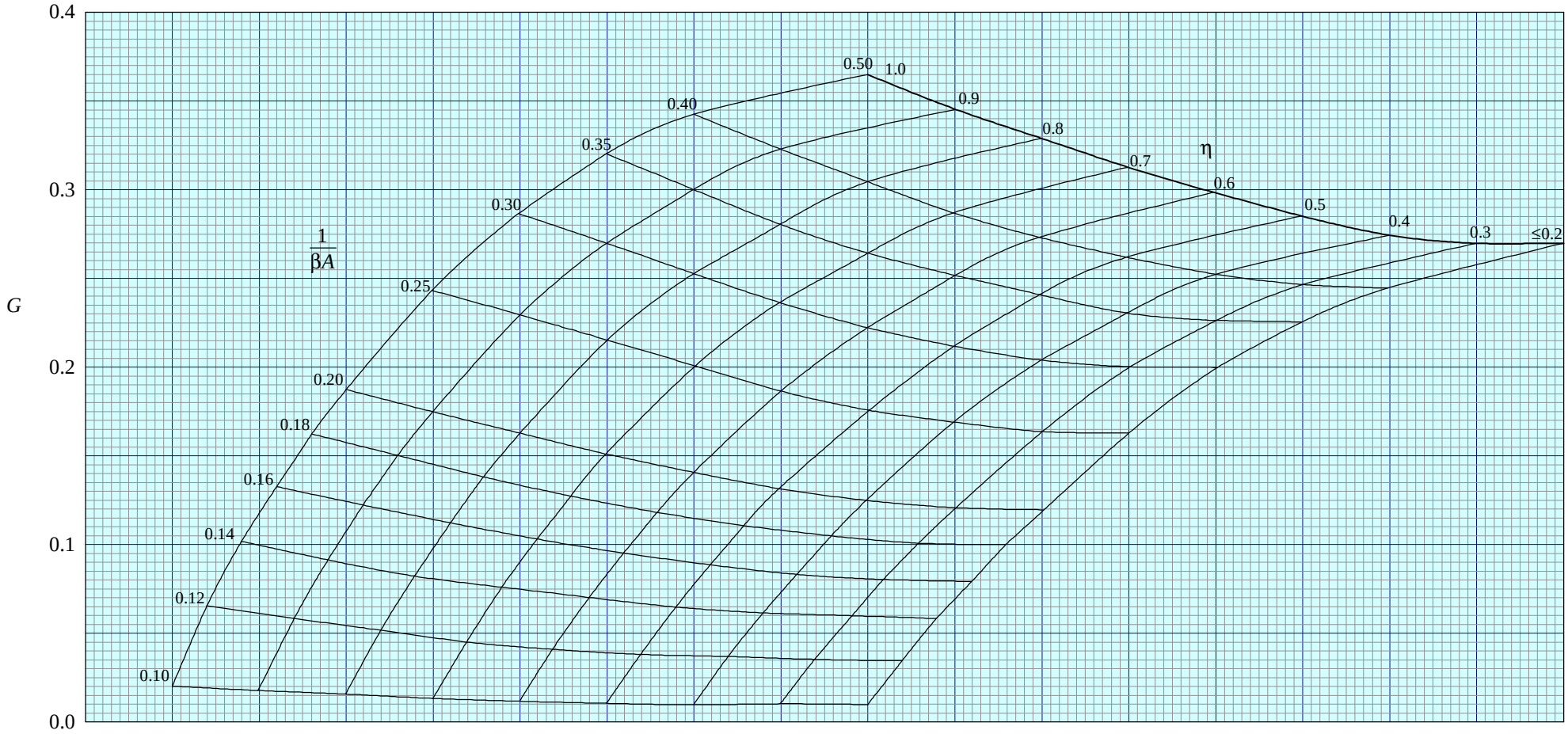

FIGURE 1c FUNCTION *G* FOR λ = 0.2

88029

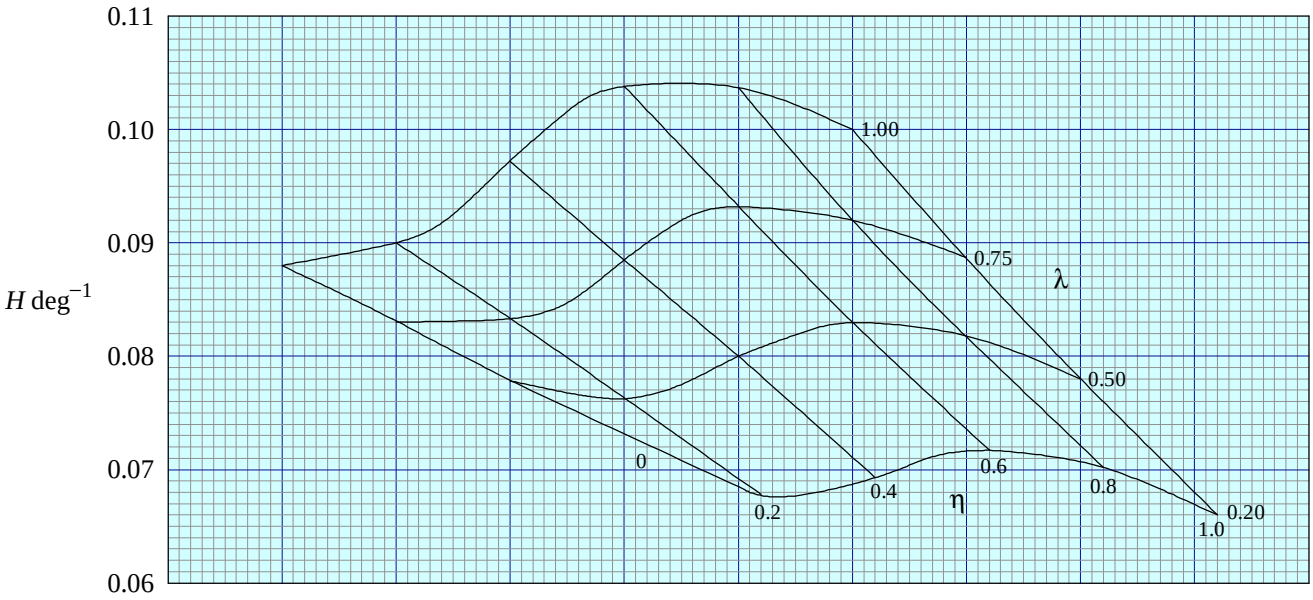

FIGURE 2 FUNCTION *H*

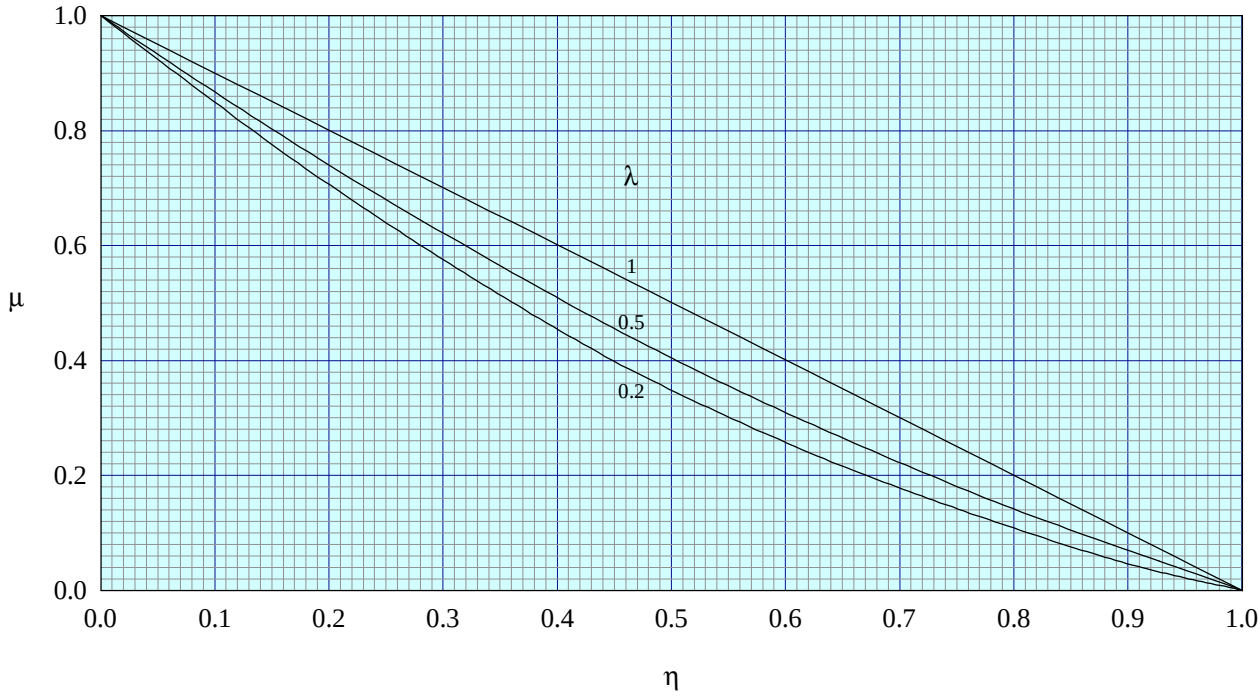

FIGURE 3 PART-SPAN FACTOR μ

THE PREPARATION OF THIS DATA ITEM

The work on this particular Item was monitored and guided by the Aerodynamics Committee which first met in 1942 and now has the following membership:

Chairman

Mr. H.C. Garner	–	Independent

Vice-Chairman

Mr. P.K. Jones	–	British Aerospace Regional Aircraft Ltd, Woodford

Members

Mr. G.E. Bean*	–	Boeing Aerospace Company, Seattle, Wash., USA
Dr. N.T. Birch	–	Rolls-Royce plc, Derby
Mr. K. Burgin	–	Southampton University
Mr D. Choo*	–	Northrop Corporation, Pico Rivera, Calif., USA
Dr T.J. Cummings	–	Short Brothers plc
Mr J.R.J. Dovey	–	Independent
Mr S.P. Fiddes	–	University of Bristol
Dr K.P. Garry	–	Cranfield Institute of Technology
Mr P.G.C. Herring	–	Sowerby Research Centre, Bristol
Mr R. Jordan	–	Aircraft Research Association
Mr K. Karling*	–	Saab-Scania, Linköping, Sweden
Mr R. Sanderson	–	Deutsche Airbus GmbH, Bremen, Germany
Mr A.E. Sewell*	–	McDonnell Douglas, Long Beach, Calif., USA
Mr M.R. Smith	–	British Aerospace Airbus Ltd, Bristol
Miss J. Willaume	–	Aérospatiale, Toulouse, France.

* Corresponding Member

The technical work in the assessment of the available information and the construction and subsequent development of the Data Item was carried out by

Mr R.W. Gilbey	–	Senior Engineer.